Chapter 4

Mesoporous Carbons for Energy-Efficient Water Splitting to Produce Pure Hydrogen at Room Temperature

Mohindar S. Seehra and Vishal Narang

Additional information is available at the end of the chapter

http://dx.doi.org/10.5772/62503

Abstract

Theoretical and experimental aspects of the use of mesoporous carbons in carbon-assisted water electrolysis (CAWE) to produce pure hydrogen at room temperature are presented. It is shown that the electrical energy requirements for CAWE can be as low as 20% of the energy needed for conventional water electrolysis, the extra energy coming from the electrochemical oxidation of carbon occurring at room temperature. Although CO_2 is produced at the anode in this process, it is well separated from pure H_2 produced at the cathode. Experimental results are reviewed for a variety of carbons with the major focus on the results obtained with carbon BP2000, which has both mesopores and micropores and a nanocarbon produced by the hydrothermal treatment of microcrystalline cellulose.

Keywords: Hydrogen, Carbons, Electrolysis, Energy efficiency, Carbon dioxide

1. Introduction

Mesoporous materials with pore size from 2 to 50 nm fall in the middle range between microporous (pore size <2 nm) and macroporous (pore size >50 nm) materials. In a recent book edited by Titirici [1] and a review by Liang et al. [2], various processes for producing mesoporous carbon materials have been described. Sevilla and Fuertes [3] and Seehra et al. [4, 5] used hydrothermal treatment of cellulose and lignin to produce nanoparticles of carbon. Liu and Guo [6] compared the characteristics of carbons produced by the hydrothermal treatment of holocellulose and crude biomass. Other methods of preparing mesoporous

carbons have been reported by Zhou et al. [7] for supercapacitor applications. Such carbons produced by different methods have applications in separation processes, catalysis, energy storage (such as super capacitors), and energy conversion. A very popular commercial source of mesoporous and microporous carbons is non-graphitized Black Pearls (BP) carbon blacks manufactured by Cabot Corporation. The pore structures of the BP carbons have been reported by Kruk et al. [8].

The focus of this review is on the use and the science of mesoporous/microporous carbons for the electrochemical production of pure hydrogen at room temperature employing electrical energy as low as 20% of the energy used in ordinary water electrolysis (WE). This process was first proposed and demonstrated by Coughlin and Farooque [9, 10] and developed more fully in the recent investigations of Seehra et al. using a variety of carbons and termed as carbon-assisted water electrolysis (CAWE) [11, 12]. Some follow-up studies of this process have been reported by Dubey et al. [13] using a carbon nanotube anode and by Giddy et al. [14] using a solid-state electrolytic cell. A different variation of this process involving hydrogen generation by laser irradiation of a carbon powder suspension in water has been reported by Akimoto et al. [15]. Results of the hydrogen evolution rate R_H using a variety of carbons show some proportionality to the surface area of a carbon which in turn is related to the pore structure of the carbons. The best results so far have been obtained with carbon BP2000, which as shown later has both micropores and mesopores and a surface area of about 1500 m^2/g.

This review covers the science behind CAWE followed by select experimental results and a comparative energy analysis of the process vis-à-vis conventional WE. Such comparative energy assessment of different processes to produce H_2 is essential for considering practical applications of the different processes. The remaining sections are organized as follows. In Section 2, prominent analytical techniques used in the structural characterization of porous carbons are reviewed with some examples imported from the published literature. Section 3 deals with the science behind CAWE and the experimental results on the electrochemical production of hydrogen reported in the literature using different carbons. The comparative energy analysis of the CAWE and WE processes is presented in Section 4. Concluding remarks of this review are given in Section 5.

2. Structural characterization of porous carbons

The porous structure of materials is often determined by means of adsorption of gases such as nitrogen and argon over a wide range of pressures. For activated carbons, the resulting structure depends on the process of activation, the activation agent, and the nature of the raw material used for producing a carbon. Kruk et al. [8] reported the surface and structural parameters (standard BET surface area S_{BET}, external surface area S_{ex}, micropore volume V_{mi}, and total pore volume V_t) of six carbon blacks produced by Cabot Corporation. These are named as Cabot BP120, BP280, BP460, BP800, BP1300, and BP2000 with S_{BET} = 30, 41, 78, 242, 520, and 1450 m^2/g, respectively. The pore volume distribution of these six carbons determined from nitrogen adsorption and desorption isotherms at 77.35 K and reproduced from Ref. [8]

http://dx.doi.org/10.5772/62503

is shown in **Figure 1**. From these graphs, it is evident that BP 120 and BP 280 have only small amount of pores, mostly in macroregion. BP460 has some mesoporosity, whereas BP800 and BP1300 are largely mesoporous with some microporosity. In contrast, BP2000 contains large fraction of micropores in addition to mesopores and some macropores. The ratio of S_{BET}/V_t for BP120, BP280, BP460, BP800, BP1300, and BP2000, based on the numbers given in Ref. [8] are 375, 410, 269, 356, 571, and 829 m^2/mL, respectively, showing that shapes and sizes of the particles and pores for the BP1300 and BP 2000 are quite different from the other four carbons.

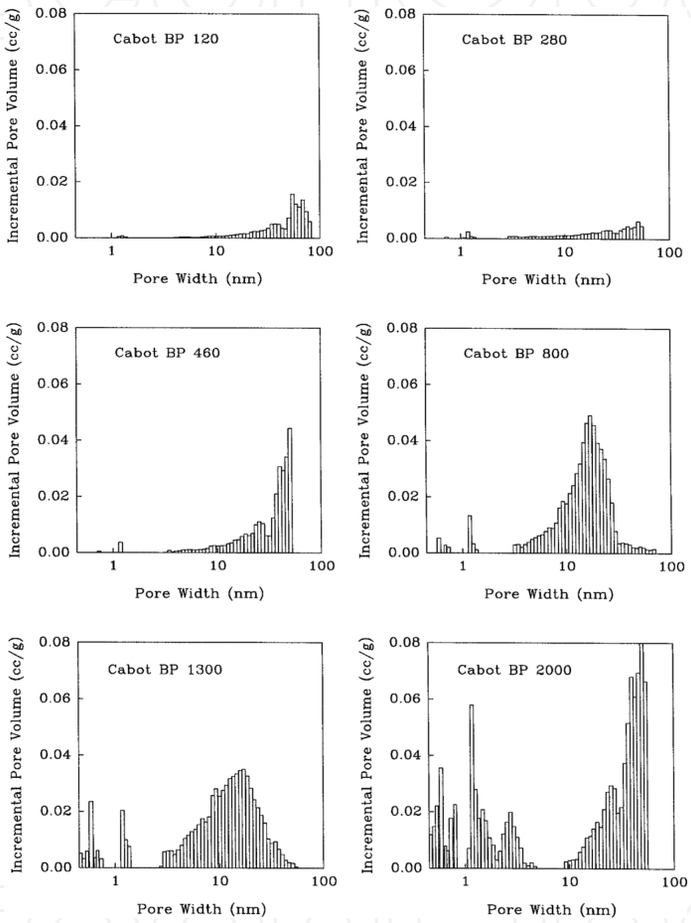

Figure 1. Pore size distribution of the six carbon blacks. (Reproduced with permission from Kruk et al. [8], copyright Elsevier 1996).

Characterization of seven activated carbons from PICA-USA for supercapacitor applications is reported by Gamby et al. [16]. Their BET surface areas ranged from a low of 1200 m^2/g to a high of S_{BET} = 2315 m^2/g. These carbons contained roughly equal fractions of microporous and mesoporous volume fractions with total porous volume ≈1 cm^3/g for pore sizes <50 nm. The microporous volume increases nearly linearly with increase in the surface area. The specific capacitance increased by about 40% with increase in S_{BET} from about 1000 m^2/g to about 2000 m^2/g. This improvement in specific capacitance was tentatively related to increase in the mesoporous volume of the carbons.

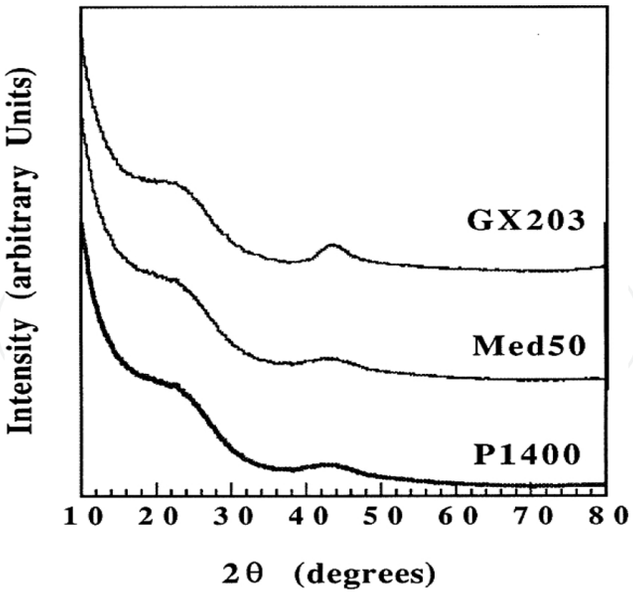

Figure 2. Wide-angle X-ray diffraction patterns of the three PICA carbons. (Reproduced with permission from Manivannan et al. [17], copyright Elsevier 1999).

Manivannan et al. [17] reported characterization of three PICA carbons viz. GX203, P1400, and Med50 with S_{BET} = 1000, 1150 and 2000 m^2/g, respectively, using the experimental techniques of wide-angle X-ray diffraction (WAXD), Raman spectroscopy, magnetometry, and electron spin resonance (ESR) spectroscopy. In **Figure 2**, we show the WAXD patterns of the three carbons using Cu-Kα source, with the broad lines near $2\theta = 24°$ and 44° due to graphitic crystallites corresponding to the (002) and (101)/(101) Bragg lines, respectively. The widths of these lines are then used to determine L_c (L_a) as the crystallite sizes along the c(a) directions, yielding $L_c \approx 1$ nm and $L_a \approx 3$ nm for these carbons. The Raman spectra of the three carbons, shown in **Figure 3**, can also be used to determine L_a from the empirical relation: L_a (nm) = 4.4/R, where R = I(1350)/I(1600) is the ratio of the intensities of the D band near 1350 cm^{-1} and the G band near 1600 cm^{-1}. This analysis also showed $L_a \approx 3$ nm in agreement with the results from WAXD. A similar comparison of the use of WAXD and Raman spectroscopy for characterizing carbons is given by Cuesta et al. [18]. ESR and magnetometry was used by Manivannan et al. [17] to determine the density of ESR active surface dangling bonds and nature of magnetic impurities which otherwise could not be detected by WAXD.

From the WAXD data shown in **Figure 2**, it is evident that for the lower 2θ values, the scattered intensity of X-ray photons increases sharply with decrease in 2θ. This is a characteristic feature of many amorphous materials. Measurements of the intensity of scattered X-rays covering smaller angles from $2\theta = 0.1°$ to 10° are termed small angle X-ray scattering (SAXS), and it can provide very useful information about pore sizes and structural aspects of macromolecules between 5 and 25 nm. In this case, the quantity plotted is the intensity I(q) of the scattered X-rays of wavelength λ as a function of momentum transfer $q = 4\pi \cdot \sin\theta/\lambda$ and such a plot can separate out contributions from micro and macropores [19]. In general, the intensity $I(q) \sim q^{-\alpha}$ where $\alpha = 6-D$, with D being the dimensionality of pore-boundary surface [20]. Experiments of SAXS in a lignite coal showed $\alpha = 3.5$ and so D = 2.5 signifying fractal nature of the surface.

http://dx.doi.org/10.5772/62503

Peaks in the I(q) versus q provides information on the size of macromolecules as for example observed in carbon nanotube suspensions [21].

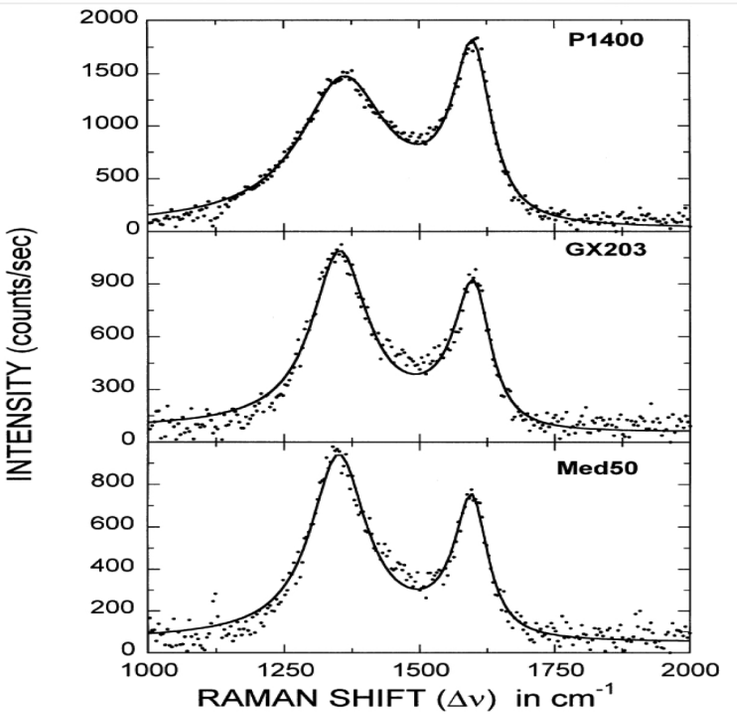

Figure 3. Raman spectra of the three PICA carbons. (Reproduced with permission from Manivannan et al. [17], copyright Elsevier 1999).

Techniques other than those described above that have also been used for the characterization of carbons include Fourier transform infrared (FTIR) spectroscopy, thermogravimetric analysis (TGA), X-ray photoelectron spectroscopy (XPS), scanning electron microscopy (SEM), and transmission electron microscopy (TEM). FTIR spectroscopy is particularly useful for determining the nature of surface functional groups. The use of all these techniques except XPS was employed in the characterization of the carbons produced from the hydrothermal carbonization of microcrystalline cellulose [4]. SEM/TEM is indispensable tools for visualization of the size and morphology of the particles [1–5], and TGA provides good information on the decomposition and oxidation characteristics of carbons [4]. The technique of XPS is often used for determining the elemental composition of a material. In summary, techniques that are used for structural characterization of other materials can also be used for carbons.

3. Carbon-assisted WE

The basic reactions for the well-known process of WE and Carbon-assisted water electrolysis (CAWE), the latter proposed by Coughlin and Farooque [9, 10], are given below:

3.1. Water electrolysis (WE)

$$\text{Anode: } 2H_2O \rightarrow O_2 + 4H^+ + 4e^- \tag{1}$$

$$\text{Cathode: } 4H^+ + 4e^- \rightarrow 2H_2 \tag{2}$$

$$\text{Net reaction: } 2H_2O \rightarrow 2H_2 + O_2 \tag{3}$$

3.2. Carbon-assisted water electrolysis (CAWE)

$$\text{Anode: } C(s) + 2H_2O \rightarrow CO_2 + 4H^+ + 4e^- \tag{4}$$

$$\text{Cathode: } 4H^+ + 4e^- \rightarrow 2H_2(g) \tag{5}$$

$$\text{Net reaction: } C(s) + 2H_2O(l) \rightarrow CO_2(g) + 2H_2(g) \tag{6}$$

To understand why CAWE is more energy efficient than WE, the change in the Gibbs-free energy $\Delta G = \Delta H - T\Delta S$ needs to be determined where ΔH (ΔS) is the change in enthalpy (entropy) of the system at temperature T. This is valid for the reactions under constant temperature and constant pressure conditions. Enthalpy is best understood as standard heat of formation of a compound from its basic elements at 25°C, the enthalpy being zero for the elements. For a compound to be stable, ΔH has to be negative. A reaction is favored if $\Delta G = \Delta G$ (products) − ΔG (reactants) < 0 which implies that a reaction is favored if, $\Delta H < 0$ and $\Delta S > 0$. We now apply these concepts to reactions for WE and CAWE listed in Eqs. (1)–(6).

At 25°C, ΔH (*l*) = −68.32 kcal/mol for water and ΔH (*g*) = −94.05 kcal/mol for CO_2 [22]. The standard molar entropies (in units of cal/mol K) are 31.2, 49.0, 16.7, and 51.0 for $H_2(g)$, $O_2(g)$, $H_2O(l)$, and $CO_2(g)$, respectively. Using these numbers for reaction (3) gives ΔH = 136.64 kcal and $T\Delta S$ = 23.23 kcal for 298 K, yielding $\Delta G = \Delta H - T\Delta S$ = 113.41 kcal > 0. ΔG being >0 means that the reaction (3) is not favored and energy must be supplied to split water into H_2 and O_2. Finally, ΔG is related to the electrical potential E^o generated in the reaction by the relation [22]:

$$\Delta G = -nFE^o \tag{7}$$

Here, n is the number of electrons involved in the reaction and F = 96484.56 C/mol is the Faraday constant. For WE, n = 4 according to Eq. (1) leading to E^o = −1.23 V. The negative sign implies that a minimum of E^o = 1.23 V must be applied to split water. Note that we have used 1 cal = 4.184 J and volt = Joules /Coulomb.

http://dx.doi.org/10.5772/62503

For CAWE, defined by reaction (6), a similar analysis yields $\Delta H = 42.59$ kcal, $\Delta S = 80.05$ cal leading to $\Delta G = 18.74$ kcal and $E^o = -0.20$ V. This suggests that for reaction (6) to proceed, a minimum $E^o = 0.20$ V needs to be applied which is a factor of $1.23/0.20 \simeq 6$ smaller than that needed for reaction (3) of WE. This extra energy comes from carbon which gets oxidized to CO_2 in the process, making CAWE six times more energy efficient than WE, at least theoretically. This process of CAWE may thus be classified as electrochemical gasification of carbon at room temperature producing pure H_2 at the cathode which is well separated from pure CO_2 produced at the anode.

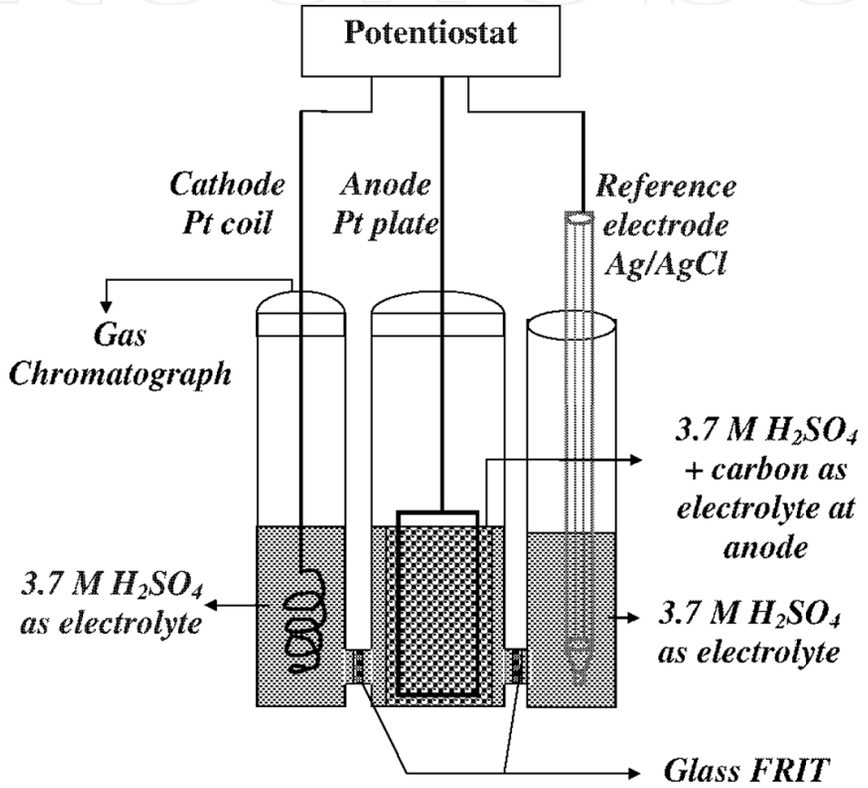

Figure 4. A schematic diagram of the three-electrode cell with Pt plate as anode (surface area = 6.8 cm^2) and Pt coil as cathode (surface area = 2.5 cm^2). A magnetic stirrer was used to stir the contents of the anode. (Reproduced with permission from Seehra et al. [11], copyright AIP Publishing LLC 2007).

Experimentally, an electrochemical cell of the type shown in **Figure 4** is often used. Because of the over-potentials of the electrodes which are related to their intrinsic properties and surface structure, E^o considerably greater than the theoretical 1.23 V in WE and the theoretical 0.20 V in CAWE needs to be applied to initiate H_2 evolution. Electrodes made of Pt and Pd are often used because they have the lowest over-potentials [23]. For each applied voltage E^o between the cathode and the anode, the quantities measured are as follows: (i) current I_o; (ii) the time t_H needed to produce the same amounts of H_2 for each E^o as measured by gas chromatography; and the computed quantities such as the hydrogen evolution rate $R_H = 1/t_H$ and the efficiency factor $A_H = R_H/E^oI_o$ representing evolved H_2 per kWh of energy used. The voltage E^o is with respect to the standard hydrogen electrode (SHE), and it is determined from

the Eq.: $E^o = E(P) + 0.22$ V where E(P) is the voltage measured by the potentiostat with respect to the reference electrode Ag/AgCl with $E^o = 0.22$ V (SHE). It is noted that in many publications, voltages listed are simply E(P), and this needs to be kept in mind while comparing with the theoretical estimates.

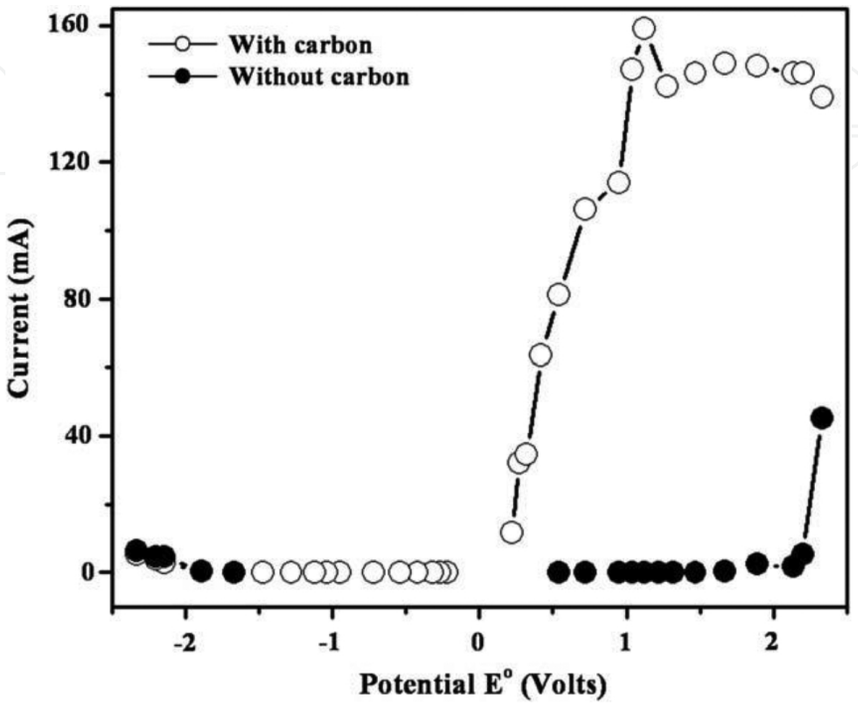

Figure 5. Forward and reverse current–voltage characteristics of the reaction, with and without adding carbon BP2000. (Reproduced with permission from Seehra and Bollineni [12], copyright Elsevier 2009).

In **Figure 5**, the effect of adding carbon BP2000 to the anode in the amount of 0.08 gm/cm^3 of the electrolyte (3.7 M H_2SO_4) is shown in terms of current–voltage plot. Without added carbon, an increase in current indicative of the start of WE only begins for $E^o > 2$ V. With the addition of carbon BP2000 to the anode, a rapid increase in current accompanied by evolution of H_2 gas at the cathode was observed for $E^o > 0.4$ V. These results are consistent with the theoretical predictions mentioned earlier in that the presence of carbon in the anode significantly lowers the threshold voltage to initiate WE and produce H_2 gas at the cathode.

It is noted that 3.7 M H_2SO_4 is chosen for the electrolyte since this particular concentration was found to have the highest electrical conductivity [10]. Similarly, the carbon concentration of 0.08 g/cm^3 was determined to be most efficient and practical by varying the concentration of the added carbon [11, 12]. A number of carbons were tried for their effects on the hydrogen generation rate R_H (**Figure 6**). As evident in **Figure 6**, carbon BP2000 yielded the best R_H values and so most of the follow up experiments were made with carbon BP2000 [12]. Another carbon that produced similar R_H values was the carbon produced by the hydrothermal treatment of microcrystalline cellulose using water as solvent and treated at 250°C for 60 min under the maximum pressure of 800 psi. This hydrothermal carbonization yielded spherical carbon particles of about 210 nm [4]. In the following section, the results obtained with carbon BP2000

http://dx.doi.org/10.5772/62503

[12] and hydrothermally treated cellulose are compared. The liquid-phase products obtained in the hydrothermal treatment of microcrystalline cellulose have also been analyzed [24].

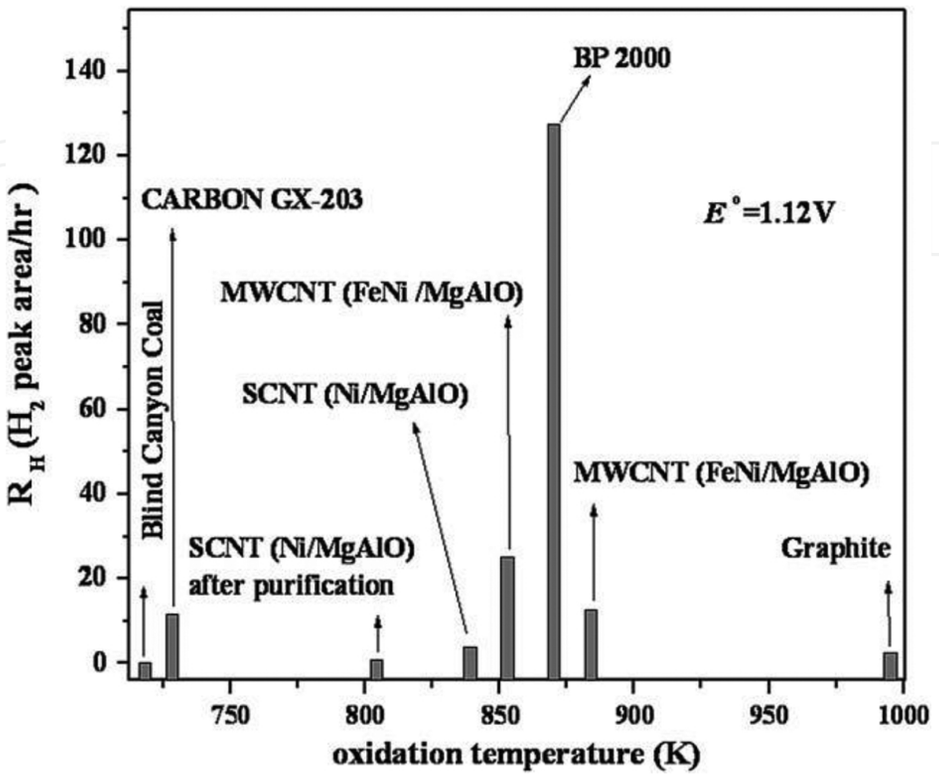

Figure 6. Comparison of hydrogen evolution rate R_H measured at E^o = 1.12 V for several carbons plotted vs. oxidation temperatures of carbons determined by thermo-gravimetric analysis. MWCNT and SCNT stand for multi-walled and single-walled carbon nanotubes, respectively (Reproduced with permission from Seehra and Bollineni [12], copyright Elsevier 2009).

In the experiments reported in Refs. [4] and [12], H_2 was produced electrochemically first by conventional WE using 3.7 M H_2SO_4 as the electrolyte and then by adding carbons and cellulose-derived nanocarbons to the anode in separate experiments, repeating the experiments each time by measuring current I_o and hydrogen solution rate R_H as a function of the voltage E^o applied between the cathode and anode. Evolved hydrogen at the cathode was measured by a calibrated gas chromatograph. The efficiency factor $A_H = R_H/E^o I_o$ representing evolved H_2 per kWh of energy used is then computed for each E^o. The plots of current in the circuit, R_H and A_H as a function of applied voltage E^o (relative to the SHE) are shown in **Figure 7** for three cases: (i) electrolyte only, (ii) carbon BP2000 added to the anode in the amount of 0.08 gm/mL of the electrolyte, and (iii) the carbon produced by the hydrothermal treatment of cellulose added to the anode in the amount of 0.08 gm/mL of the electrolyte. In the WE process, a noticeable current and R_H is observed only if $E^o > 2$ V. However, for both BP2000 and hydrothermally treated cellulose, significant I_o and R_H are observed at E^o = 0.7 V. In **Figure 7**, the horizontal dotted line is drawn to show that using commercial carbon BP2000 with surface area of 1500 m^2/g, same R_H is obtained at applied voltage E^o = 0.7 V using carbon BP2000 as obtained by applying E^o = 2.6 V in conventional WE. For carbon produced by hydrothermal

treatment of cellulose, E^o = 1.2 V is needed to produce the same R_H. A detailed analysis of the comparison of the efficiencies of the three processes is given in Section 4.

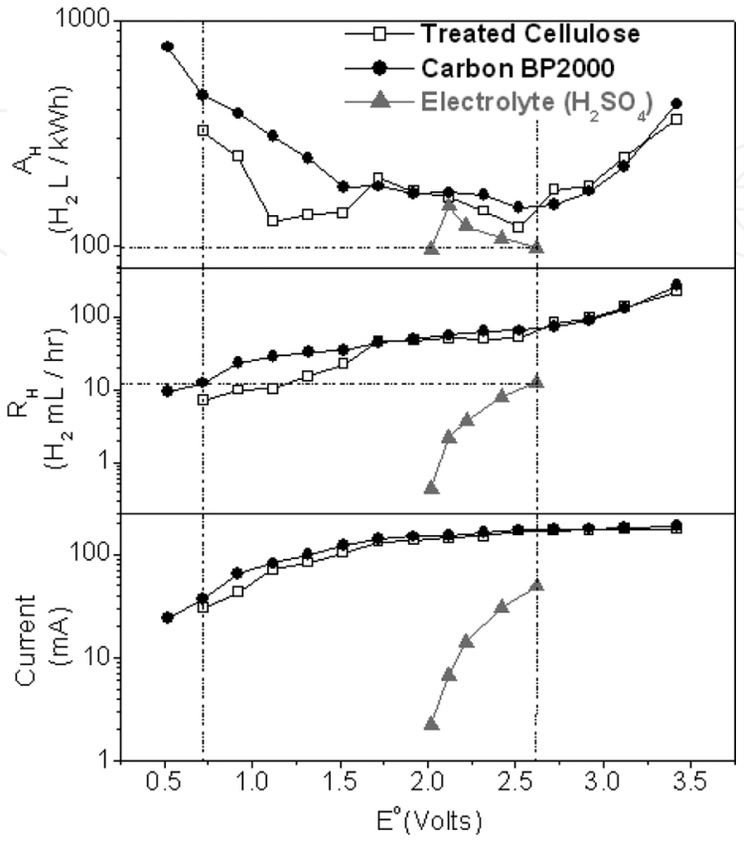

Figure 7. Comparison of current, hydrogen evolution rate R_H, and efficiency factor A_H against applied voltage E^o (vs. standard hydrogen electrode) for HTP-cellulose treated at 250°C for 60 min, carbon BP2000 and electrolyte only. (Reproduced with permission from Seehra et al. [4], copyright Elsevier 2012).

According to the Eqs. (4) and (5) valid for CAWE, H_2 should be produced at the cathode and CO_2 at the anode in the molar ratio of H_2/CO_2 =2. With careful quantitative measurements, this indeed was found to be valid using carbon BP2000 [12]. However, using carbon produced from the hydrothermal treatment of cellulose, CO_2 at the anode could not be detected with certainty suggesting that the reaction with this carbon is more complicated perhaps because of the presence of surface group present in this carbon [4]. Another difficulty in the quantification of CO_2 is that its peak in gas chromatography is quite weak relative to peaks from H_2 and O_2. Regardless, CO_2 produced in CAWE at the anode is well separated from H_2 produced at the cathode. This is important since CO_2 is a green-house gas and so it can be collected in relatively pure form and so appropriately used or sequestered.

Of all the carbons results for which are shown in **Figure 6**, BP2000 was found to be the most efficient for producing H_2. It is very likely that this is due to surface area effect since BP2000 has high surface area of 1500 m^2/g. However, a direct correlation between the surface area and R_H has not yet been established experimentally. It may be possible to do so by comparing R_H yields for the various BP carbons with different surface areas shown in **Figure 1**.

http://dx.doi.org/10.5772/62503

4. Comparative energy analysis

Understanding the efficiencies of various processes to produce hydrogen is very important for practical considerations. In this regard, Rosen and Scott [25] have published a comparative energy analysis of the various processes currently in use for producing H_2. The summary of this analysis, reproduced from their paper, is given in **Table 1**. According to this analysis, the energy efficiency of the conventional WE for producing H_2 gas is only about 30% compared to about 85% for the steam methane reforming (SMR) and about 60% for coal gasification (CG) processes. If heat losses to the environment are also included (exergy) in the analysis, then these efficiencies are reduced by an additional few percent. The energy efficiency here is defined as the ratio of the energy contained in the produced hydrogen to the input energy. Because of the higher efficiencies of the SMR and CG processes, these are currently the favored techniques for producing H_2 although both of these processes also produce CO_2.

Category	Process	Efficiency (%)	
		Energy	Exergy
Hydrocarbon-based	Steam-methane reforming (SMR)	86	78
	Coal gasification	59	49
Non-hydrocarbon-based	Current-technology water electrolysis	30	26
	Advanced-technology water electrolysis	49	41
	Thermochemical water decomposition	21	19
Integrated	SMR/current-technology water electrolysis	55	48
	SMR/advanced-technology water electrolysis	70	62
	SMR/thermochemical water decomposition	45	40

Reproduced with permission from Rosen and Scott [25] copyright Elsevier 1998

Table 1. Hydrogen production processes and their efficiencies considering fuel and/or a hypothetical heat source as the external energy inputs.

In the recent paper [4], energy efficiencies of the WE and CAWE processes were considered in terms of the energy equivalence of electrical energy in kWh (kilo-watt-hour) and liters (L) of produced H_2. Using the data available in the literature, it can be shown that one gasoline gallon equivalent (GGE) equals 33.4 kWh of electricity which in turn equals 10.1 m^3 of H_2 gas at STP (standard temperature and pressure). According to this equivalence, one kWh of electricity equals 300 L (liters) of hydrogen implying that one kWh of electricity used in electrolysis must produce 300 L of H_2 @ STP for 100% energy efficiency. This equivalence is used here to determine the energy efficiencies of WE and CAWE processes, the latter using carbon BP2000 and the carbon produced from the hydrothermal treatment of microcrystalline cellulose [4].

Examining the results shown in **Figure 7**, it is evident that for electrolyte only representing conventional WE, $E^o > 2$ V is needed to start the reaction, reaching close to saturation at $E^o =$

2.6 V. At this voltage, R_H is about 15 mL/h of hydrogen and A_H equals 100 L of H_2 produced per kWh of electrical energy used. As noted earlier, if process was 100% energy efficient, A_H = 300 L/kWh should have been produced. Thus, conventional WE is only about 33% (100/300) efficient, in close agreements with the results from the analysis of Rosen and Scott shown in **Table 1**.

Following the horizontal dotted line drawn in **Figure 7**, it is evident that using commercial carbon BP2000 with surface area of 1500 m^2/g, same R_H is obtained at applied voltage E^o = 0.7 V using carbon BP2000 as obtained by applying E^o = 2.6 V in conventional WE. However, at E^o = 0.7 V with carbon BP2000, A_H = 450 L/kWh of H_2 is produced resulting in energy efficiency of 150% (450/300) compared to about 33% for conventional WE. This extra energy representing nearly fivefold improvement in energy efficiency over conventional WE is coming from the extra electrons provided by use of carbon BP2000. This electrochemical gasification occurring at room temperature does produce CO_2 at the anode, but it is well separated from the H_2 produced at the cathode.

In **Figure 7**, the data of H_2 production using carbon produced from hydrothermally treated cellulose instead of carbon BP2000 is also shown. With the use of carbon produced from hydrothermally treated cellulose, again following the horizontal line, somewhat lower $A_H \simeq$ 350 L/kWh is obtained at E^o = 0.7 V with essentially similar evolution rate R_H of H_2. This yields slightly lower energy efficiency of about 120% (350/300) which is still a factor of four improvement over conventional WE. This electrochemical process with cellulose-derived nanocarbon has the added advantage that no CO_2 could be detected at the anode presumably because cellulose-derived nanocarbons have surface functional groups [4] unlike carbon BP2000. It is noted that in doing these comparisons of energy efficiencies, the cost of producing the carbons is not included. However, BP2000 is available commercially in large quantities and hydrothermal carbonization is environmentally friendly process employing water as solvent under subcritical temperature–pressure conditions [24].

In summary, the comparative energy analysis described here shows factors of four to five improvements in the energy efficiencies for producing H_2 electrochemically using commercial carbon BP2000 and cellulose-derived nanocarbons. Pure CO_2 is produced with the use of carbon BP2000, but it is well separated from H_2. The use of post-HTP cellulose has the advantage that no CO_2 could be detected in the process. For more practical issues related to the electrochemical production of hydrogen from WE, the reader is referred to the recent review by Wang et al. [23].

5. Concluding remarks

In this review, the focus has been on just one application of mesoporous/microporous carbons viz. in CAWE to produce H_2 at energy-efficient voltages. Theoretical considerations and experimental results have established that the electrical energy requirements for CAWE are a factor of about five smaller than those needed for conventional WE. CO_2 is produced at the cathode in CAWE resulting from the room temperature oxidation of carbon. However, it is

http://dx.doi.org/10.5772/62503

well separated from pure H_2 produced at the anode. Whether this energy advantage of CAWE vis-à-vis conventional WE can be commercially exploited still remain to be seen since there are often other technical issues that must be overcome as described in the recent review of Wang et al. [23]. Comparing the results in **Figure 6** obtained with the use of a variety of carbons, it is evident that the best H_2 evolution rate R_H was obtained using carbon BP2000 with high surface area of about 1500 m^2/g. Since smaller pore size leads to higher surface area, a correlation quite likely exists between R_H and pore size of the carbons. Additional studies along these lines using different carbons with known pore-size structure and surface areas might be fruitful. As mentioned in the Introduction, there are of course many other applications of mesoporous and microporous carbons and some of these are addressed in the other chapters of this book.

Author details

Mohindar S. Seehra* and Vishal Narang

*Address all correspondence to: mseehra@wvu.edu

Department of Physics and Astronomy, West Virginia University, Morgantown, USA

References

[1] Titirici M.-M., *Sustainable carbon materials from hydrothermal processes*. Wiley Online Library, 2013.

[2] Liang C., Li Z., and Dai S., *Mesoporous carbon materials: synthesis and modification*. Angewandte Chemie International Edition, 2008. 47(20): 3696–3717.

[3] Sevilla M., and Fuertes A.B., *The production of carbon materials by hydrothermal carbonization of cellulose*. Carbon, 2009. 47(9): 2281–2289.

[4] Seehra M., Akkineni L., Yalamanchi M., Singh V., and Poston J., *Structural characteristics of nanoparticles produced by hydrothermal pretreatment of cellulose and their applications for electrochemical hydrogen generation*. International Journal of Hydrogen Energy, 2012. 37(12): 9514–9523.

[5] Seehra M.S., Pyapalli S.K., Poston J., Atta-Obeng E., and Dawson-Andoh B., *Hydrothermal conversion of commercial lignin to carbonaceous materials*. Journal of the Indian Academy of Wood Science, 2015. 12(1): 29–36.

[6] Liu F., and Guo M., *Comparison of the characteristics of hydrothermal carbons derived from holocellulose and crude biomass*. Journal of Material Science, 2015. 50: 1624–1631.

[7] Zhou D.-D., Du Y.-J., Song Y.-F., Wang Y.-G., Wang C.-X., and Xia Y.-Y., *Ordered hierarchical mesoporous/microporous carbon with optimized pore structure for supercapacitors*. Journal of Materials Chemistry A, 2013. 1(4): 1192–1200.

[8] Kruk M., Jaroniec M., and Bereznitski Y., *Adsorption Study of Porous Structure Development in Carbon Blacks*. Journal of Colloid and Interface Science, 1996. 182(1): 282–288.

[9] Coughlin R.W., and Farooque M., *Hydrogen production from coal, water and electrons*. Nature, 1979. 279(5711): 301–303.

[10] Coughlin R.W., and Farooque M., *Electrochemical gasification of coal-simultaneous production of hydrogen and carbon dioxide by a single reaction involving coal, water, and electrons*. Industrial & Engineering Chemistry Process Design and Development, 1980. 19(2): 211–219.

[11] Seehra M., Ranganathan S., and Manivannan A., *Carbon-assisted water electrolysis*: *an energy-efficient process to produce pure H_2 at room temperature*. Applied Physics Letters, 2007. 90(4): 044104; ibid 2008, 92, 239902.

[12] Seehra M., and Bollineni S., *Nanocarbon boosts energy-efficient hydrogen production in carbon-assisted water electrolysis*. International Journal of Hydrogen Energy, 2009. 34(15): 6078–6084.

[13] Dubey P.K., Sinha A.S.K., Talapatra S., Koratkar N., Ajayan P.M., and Srivastava O.N., *Hydogen generation by water electrolysis using carbon nanotube anode*, International Journal of Hydrogen Energy, 2010. 35: 3945–3950.

[14] Giddy S., Kulkarni A., and Badwal S. P. S., *Low emission hydrogen generation through carbon assisted electrolysis*, International Journal of Hydrogen Energy, 2015. 40: 70–74.

[15] Akimoto I., Maeda K., and Ozaki N., *Hydrogen generation by laser irradiation of carbon powder in water*, Journal of Physical Chemistry C, 2013. 117: 18281–18285.

[16] Gamby J., Taberna P.L., Simon P., Fauvarque J.F., and Chesneau M., *Studies and characterisations of various activated carbons used for carbon/carbon supercapacitors*. Journal of Power Sources, 2001. 101(1): 109–116.

[17] Manivannan A., Chirila M., Giles N., and Seehra M., *Microstructure, dangling bonds and impurities in activated carbons*. Carbon, 1999. 37(11): 1741–1747.

[18] Cuesta A., Dhamelincourt P., Laureyns J., Martinez-Alonso A., and Tascon J.M., *Comparative performance of X-ray diffraction and Raman microprobe techniques for the study of carbon materials*. Journal of Materials Chemistry, 1998. 8(12): 2875–2879.

[19] Gibaud A., Xue J., and Dahn J., *A small angle X-ray scattering study of carbons made from pyrolyzed sugar*. Carbon, 1996. 34(4): 499–503.

[20] Bale H.D., and Schmidt P.W., *Small-angle X-ray-scattering investigation of submicroscopic porosity with fractal properties*. Physical Review Letters, 1984. 53(6): 596–599.

[21] Zhou W., Islam M., Wang H., Ho D., Yodh A., Winey K.I., and Fischer J.E., *Small angle neutron scattering from single-wall carbon nanotube suspensions*: *evidence for isolated rigid rods and rod networks*. Chemical Physics Letters, 2004. 384: 185–189.

[22] Roberts E.K., *Principles of Physical Chemistry*. Allyn & Bacon, Boston, USA, 1984.

[23] Wang M., Wang Z., Gong X., and Guo Z., *The intensification technologies to water electrolysis for hydrogen production–a review*. Renewable and Sustainable Energy Reviews, 2014. 29: 573–588.

[24] Seehra M., Popp B., Goulay F., Pyapalli S., Gullion T., and Poston J., *Hydrothermal treatment of microcrystalline cellulose under mild conditions*: *characterization of solid and liquid-phase products*. Cellulose, 2014. 21(6): 4483–4495.

[25] Rosen M.A., and Scott D.S., *Comparative efficiency assessments for a range of hydrogen production processes*. International Journal of Hydrogen Energy, 1998. 23: 653–659.

IntechOpen